

Article

Free Vibration Analysis of Three Layered Beams with a Soft-Core Using the Transfer Matrix Method

Jung Woo Lee

Department of Mechanical System Engineering, Kyonggi University, 154-42, Gwanggyosan-ro, Yeongtong-gu, Suwon-si 16227, Gyeonggi-do, Republic of Korea; j.w.lee@kyonggi.ac.kr; Tel.: +82-31-249-9819; Fax: +82-31-244-6300

Abstract: In this study, the free vibration characteristics of symmetric three-layered beams with a soft core, whereby the mass of the core could be ignored, were investigated. The coupling effect of the axial and bending displacements owing to the presence of the soft core was considered. Classical beam theory was employed for analyzing the top and bottom layers, and only the shear deformation was applied for the core layer. The frequency determinant was deduced using the transfer matrix method. The efficacy of the method was demonstrated through a comparison with the natural frequencies obtained in previous studies. To determine the physical phenomena caused by the exchange process in the order of modes of such beams, a new analytical method is proposed. As an example, the dynamic behavior of a three-layered beam was analyzed by examining the changes in the strain energies related to the natural frequencies and mode shapes. All bending-dominated modes were accompanied by the axial displacements because of the existence of a core layer, whereas the axial-dominated modes were uncoupled with the bending displacements. In addition, the efficiency of the proposed method was demonstrated through relevant discussions of the predicted results.

Keywords: soft-core; three-layered beam; transfer matrix method; free vibration analysis



Citation: Lee, J.W. Free Vibration Analysis of Three Layered Beams with a Soft-Core Using the Transfer Matrix Method. *Appl. Sci.* **2023**, *13*, 411. <https://doi.org/10.3390/app13010411>

Academic Editor: Junhong Park

Received: 5 December 2022

Revised: 22 December 2022

Accepted: 26 December 2022

Published: 28 December 2022



Copyright: © 2022 by the author. Licensee MDPI, Basel, Switzerland. This article is an open access article distributed under the terms and conditions of the Creative Commons Attribution (CC BY) license (<https://creativecommons.org/licenses/by/4.0/>).

1. Introduction

Sandwich structures with strength-to-weight ratios have been widely applied in fields, such as conveying structures, aeronautics, and astronautics. A three-layer sandwich beam is usually composed of a top face, core made of lightweight materials, and bottom face layers [1–5]. Investigating the dynamic characteristics of sandwich beams based on the behavior of the core is important. In particular, it is necessary to analyze the dynamic behavior of the face layer in relation to that of the core layer. Dynamic behavior analysis of sandwich beams has been performed by many investigators [6–30], and advanced techniques [7–12] based on the classical sandwich beam theory have been developed for the vibration analysis of such beams.

The static analysis of sandwich beams for distributed and sinusoidal loadings using the finite element model based on the higher-order zigzag shear deformation theory was investigated [13], and a sandwich beam element was studied to design sandwich beams with partially delaminated regions [14]. Studies on the bending, buckling, and free vibration analyses of laminated sandwich beams are discussed in a review paper by Sayyad and Ghugal [15]. The effect of height-to-length ratio on the natural frequencies of three-layered sandwich beams, with different boundary conditions, was examined using higher-order zigzag beam theory [16]. The bending-dominated vibration of the soft core in the three-layer sandwich beam was analyzed using the quadrature element method [17]. The dynamic stiffness method was used to analyze the dynamic characteristics of the out-of-plane bending vibrations of symmetric sandwich beams, and they investigated the independence of the bending and torsional modes in the free vibration of such beams [18]. The effect of the ratio of core to thickness to face thickness on the natural frequencies of soft-core

sandwich beams was analyzed using tractable zig-zag beam theory [19]. A finite element model for the vibration analysis of sandwich beams with a soft core was developed by employing the Euler–Bernoulli theory for the face sheets and the Timoshenko beam theory for the core sheet [20]. The effect of the length-to-height ratio on the natural frequencies of sandwich beams with a soft core was studied using the zig-zag beam theory [21]. The dynamic behaviors of axially moving sandwich beams with a soft core were studied using the Galerkin method and complex mode method, which considered only the shear deformation for the core layer of such beams [22]. The effects of the core thickness and Poisson’s ratio on the dynamic characteristics of sandwich beams were analyzed using Kriging-based finite element models based on different shear deformation theories [23]. The effect of thickness ratios and density ratios between the face and core layers on the natural frequencies of sandwich beams is investigated by obtaining the discrete solution of the differential equation using the Green function [24], the finite element method [25], and the Chebyshev series [27], as well as by analyzing the dynamic behaviors of sandwich beams in the core layer with the dynamic stiffness method, whereby the effect of bending displacements is neglected and only shear deformation is considered [26]. The problems presented in this study are similar to those considered in [24–27]; however, the physical phenomena that were not discussed in previous studies have been analyzed using an analytical method that has been developed in the present study. The axial, bending, and shear deformations in all layers were considered in analyzing the natural frequencies and mode shapes of the sandwich beams [28]; yet, the method can be used in a limited manner for simply supported sandwich beams, and a fourth-order uncoupled governing equation was used. However, the proposed method uses a sixth-order coupled differential equation, and the present method can efficiently analyze the dynamic characteristics of such structures for various boundary conditions. Moreover, a numerical method that can accurately analyze the axial displacement effect on bending-dominated modes has not been studied. To reduce the model error of finite elements, modeling updating techniques based on the finite element method are being studied to predict the dynamic behavior of beam structures [29–31].

Some researchers [32–34] have analyzed the dynamic characteristics of sandwich beams using the transfer matrix method (TMM). The coupling of axial and bending displacements was not considered in [32]; a discrete lumped mass system [33] and discretized state equations [34] were used. The method proposed in this study is different from the ones used in the above studies. The stubborn shortcomings, as well as the advantages of the transfer matrix method have been discussed in previous works [35,36]. The use of a simple precaution to overcome the non-physical numerical instability occurring in the calculation of high-order frequencies is discussed [36].

This study aims to analyze the dynamic behaviors of sandwich beams with a soft core, and the natural frequencies and mode shapes of beams with different boundary conditions (i.e., clamped-free (C-F), clamped-clamped (C-C), clamped-pinned (C-P), and pinned-pinned (P-P) end conditions) were successfully computed using the transfer matrix method. The accuracy of the predicted results of the proposed method is compared with the natural frequencies obtained from earlier studies [26,27].

For the sandwich beam, it is assumed that the mass of the core layer can be ignored, and only the coupling of the axial and bending displacements is considered. The Euler–Bernoulli beam theory is used for the top and bottom face layers, and only the shear deformation is considered for the core layer. The continuity conditions between the core and face layers are as follows. The proposed beam model assumes that no delamination occurs between layers for free vibration. The bending of the core layer is caused by the bending displacements of the face layers; however, the bending stiffness of the core is ignored. Therefore, the shear deformation of the core, caused by the bending of the face layers, is assumed by making the difference in the axial displacements of the face layers. In addition, an analytical method that can distinguish the effects of the face and core strain energies on the natural frequencies of soft-core sandwich beams is proposed. This is

deduced from the relationship between the maximum normal strain and kinetic energies. Some physical phenomena related to the dynamic behavior of sandwich beams are revealed using the analytical method.

2. Theory

The schematic of a symmetric three-layered beam with a soft-core is illustrated in Figure 1, where h is the total height of the cross section, and h_f and h_c are the thicknesses of the face and core layers, respectively. The Euler–Bernoulli theory was used in the face layer, and it considers only the shear deformation in the core layer, owing to the bending of face layers. The concept of linear elasticity, which considers only the deformation in the X-Z plane, is employed. A core layer made of a lightweight material, whose mass can be ignored in comparison to those of the face layers, is assumed.

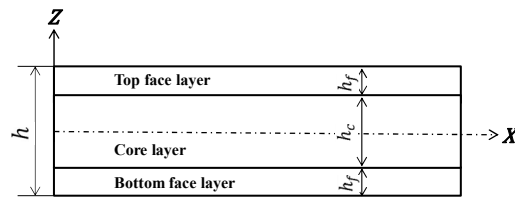


Figure 1. Schematic of a symmetric three-layered beam with a soft core.

The strain energies of the top and bottom faces can be deduced as follows [26,27]:

$$U_f = U_{f1} + U_{f2} = \frac{1}{2} E_f A_f \int_0^L 2 \left(\frac{\partial u(x,t)}{\partial x} \right)^2 dx + \frac{1}{2} E_f I_f \int_0^L 2 \left(\frac{\partial^2 w(x,t)}{\partial x^2} \right)^2 dx \quad (1)$$

where E_f , A_f , and I_f are the elastic modulus, area, and moment of inertia of the face layer, respectively. $E_f A_f$ and $E_f I_f$ are the extensional and bending rigidities in the face layer, respectively. L is the total beam length. In addition, U_{f1} is the axial strain energy, and U_{f2} is the bending strain energy. $u(x,t)$ and $w(x,t)$ are the axial and bending displacements, respectively.

The shear strain energy of the core is as follows [26,27]:

$$U_c = \frac{1}{2} k_c A_c G_c \int_0^L \left\{ \frac{2}{h_c} u(x,t) + \left(1 + \frac{h_f}{h_c} \right) \frac{\partial w(x,t)}{\partial x} \right\}^2 dx, \quad (2)$$

where k_c , A_c , and G_c are the shear correlation factor, area, and shear modulus of the core layer, respectively.

Therefore, the total normal strain energy can be expressed by

$$U = U_f + U_c \quad (3)$$

The kinetic energy of a three-layered beam with a lightweight core can be formulated as

$$\mathcal{T} = \frac{1}{2} \int_0^L 2m_f \left(\frac{\partial u(x,t)}{\partial t} \right)^2 dx + \frac{1}{2} \int_0^L 2m_f \left(\frac{\partial w(x,t)}{\partial t} \right)^2 dx, \quad (4)$$

where m_f is the mass per unit length of each face layer [26,27].

By employing Hamilton’s principle,

$$\delta \int_{t_1}^{t_2} (\mathcal{T} - U) dt = 0, \quad (5)$$

and the two differential equations, Equations (6) and (7), the bending moment and axial and shear forces can be obtained as follows [26,27]:

$$E_f A_f \frac{\partial^2 u(x, t)}{\partial x^2} - \frac{2k_c A_c G_c}{h_c^2} u(x, t) - \frac{k_c A_c G_c}{h_c} \left(1 + \frac{h_f}{h_c}\right) \frac{\partial w(x, t)}{\partial x} - m_f \frac{\partial^2 u(x, t)}{\partial t^2} = 0, \quad (6)$$

and

$$E_f I_f \frac{\partial^4 w(x, t)}{\partial x^4} - \frac{k_c A_c G_c}{2} \left(1 + \frac{h_f}{h_c}\right)^2 \frac{\partial^2 w(x, t)}{\partial x^2} - \frac{k_c A_c G_c}{h_c} \left(1 + \frac{h_f}{h_c}\right) \frac{\partial u(x, t)}{\partial x} + m_f \frac{\partial^2 w(x, t)}{\partial t^2} = 0. \quad (7)$$

Axial force,

$$F(x) = -2E_f A_f \frac{\partial u(x, t)}{\partial x}. \quad (8)$$

Bending moment,

$$M(x) = -2E_f I_f \frac{\partial^2 w(x, t)}{\partial x^2}. \quad (9)$$

Shear force,

$$V(x) = 2E_f I_f \frac{\partial^3 w(x, t)}{\partial x^3} - k_c A_c G_c \left(1 + \frac{h_f}{h_c}\right) \left\{ \left(1 + \frac{h_f}{h_c}\right) \frac{\partial w(x, t)}{\partial x} + \left(\frac{2}{h_c}\right) u(x, t) \right\}. \quad (10)$$

By assuming harmonic vibration with angular frequency (ω), the following is obtained

$$u(x, t) = U(x)e^{i\omega t}, \quad w(x, t) = W(x)e^{i\omega t}, \quad (11)$$

By substituting Equation (11) into Equations (6) and (7), the differential equations can be rewritten as

$$\frac{d^2 U(x)}{dx^2} + (b^2 - 2a^2)U(x) - a^2 c \frac{dW(x)}{dx} = 0, \quad (12)$$

$$\frac{d^4 W(x)}{dx^4} - \frac{a^2 c^2}{2r^2} \frac{d^2 W(x)}{dx^2} - \frac{a^2 c}{r^2} \frac{dU(x)}{dx} - \frac{b^2}{r^2} W(x) = 0, \quad (13)$$

where

$$a^2 = \frac{k_c A_c G_c}{E_f A_f h_c^2}, \quad b^2 = \frac{m_f \omega^2}{E_f A_f}, \quad c = (h_c + h_f), \quad r^2 = \frac{I_f}{A_f}.$$

The two differential equations can be expressed in a sixth-order differential equation:

$$\frac{d^6 \Psi(x)}{dx^6} + \alpha_1 \frac{d^4 \Psi(x)}{dx^4} + \alpha_2 \frac{d^2 \Psi(x)}{dx^2} + \alpha_3 \Psi(x) = 0, \quad (14)$$

where

$$\alpha_1 = \left(b^2 - 2a^2 - \frac{a^2 c^2}{2r^2}\right), \quad \alpha_2 = -\frac{b^2}{r^2} \left(1 + \frac{a^2 c^2}{2}\right), \quad \alpha_3 = -\frac{b^2 (b^2 - 2a^2)}{r^2},$$

and $\Psi(x) = U(x)$ or $W(x)$.

If the solution of Equation (14) is assumed to be of the form

$$\Psi(x) = He^{\lambda x}, \quad (15)$$

then, a sixth-order polynomial in λ can be obtained by substituting Equation (15) into Equation (14):

$$\lambda^6 + a\lambda^4 + b\lambda^2 + c = 0. \quad (16)$$

To determine the solution of Equation (16), this polynomial can be transformed into a third-order polynomial as follows:

$$\bar{\zeta}^3 + a\bar{\zeta}^2 + b\bar{\zeta} + c = 0, \tag{17}$$

where

$$\lambda = \pm\sqrt{\bar{\xi}}. \tag{18}$$

Thus, the displacements $U(x)$ and $W(x)$ can be defined by

$$U(x) = \sum_{j=1}^6 H_j e^{\lambda_j x}, \tag{19}$$

and

$$W(x) = \sum_{j=1}^6 Q_j e^{\lambda_j x} \tag{20}$$

where H_j and Q_j are the different constants.

The relationship between the two constants (H_j and Q_j) can be defined by substituting Equations (19) and (20) into Equation (12):

$$Q_j = \beta_j H_j, \tag{21}$$

and

$$\beta_j = \frac{\{\lambda_j^2 + (b^2 - 2a^2)\}}{a^2 c \lambda_j}. \tag{22}$$

Thus, $W(x)$ can be rewritten as

$$W(x) = \sum_{j=1}^6 \beta_j H_j e^{\lambda_j x}, \tag{23}$$

The slope of the bending deformation curve can be obtained by differentiating Equation (23) as:

$$\Phi(x) = \sum_{j=1}^6 \lambda_j \beta_j H_j e^{\lambda_j x}. \tag{24}$$

By substituting Equations (23) and (24) into Equations (8)–(10), the expression for the forces can be rewritten as

$$F(x) = -2E_f A_f \sum_{j=1}^6 \lambda_j H_j e^{\lambda_j x}, \tag{25}$$

$$M(x) = -2E_f I_f \sum_{j=1}^6 \beta_j \lambda_j^2 H_j e^{\lambda_j x}, \tag{26}$$

and

$$V(x) = E_f I_f \sum_{j=1}^6 \left\{ 2\lambda_j^3 \beta_j - \frac{a^2 c}{r^2} (c\lambda_j \beta_j + 2) \right\} H_j e^{\lambda_j x}. \tag{27}$$

The state vector $\mathbf{Z}_{x=0}$, expressed in matrix form by substituting $x = 0$ into Equations (19) and (23)–(27), is given by:

$$\mathbf{Z}_{x=0} = \mathbf{CH} \tag{28}$$

where

$$\mathbf{Z}_{x=0} = \begin{Bmatrix} U \\ W \\ \Phi \\ F \\ M \\ V \end{Bmatrix}_{x=0}, \mathbf{C} = \begin{bmatrix} C_{11} & C_{12} & C_{13} & C_{14} & C_{15} & C_{16} \\ C_{21} & C_{22} & C_{23} & C_{24} & C_{25} & C_{26} \\ C_{31} & C_{32} & C_{33} & C_{34} & C_{35} & C_{36} \\ C_{41} & C_{42} & C_{43} & C_{44} & C_{45} & C_{46} \\ C_{51} & C_{52} & C_{53} & C_{54} & C_{55} & C_{56} \\ C_{61} & C_{62} & C_{63} & C_{64} & C_{65} & C_{66} \end{bmatrix}, \mathbf{H} = \begin{Bmatrix} H_1 \\ H_2 \\ H_3 \\ H_4 \\ H_5 \\ H_6 \end{Bmatrix}, \quad (29)$$

and $C_{1j} = 1, C_{2j} = \beta_j, C_{3j} = \lambda_j \beta_j, C_{4j} = -2E_f A_f \lambda_j,$

$$C_{5j} = -2E_f I_f \beta_j \lambda_j^2, C_{6j} = E_f I_f \left\{ 2\lambda_j^3 \beta_j - \frac{a^2 c}{r^2} (c\lambda_j \beta_j + 2) \right\}.$$

From Equation (28), the constant \mathbf{H} can be obtained as follows:

$$\mathbf{H} = \mathbf{C}^{-1} \mathbf{Z}_{x=0} \quad (30)$$

Similarly, the state vector $\mathbf{Z}_{x=L}$, expressed in matrix form by substituting $x = L$ into Equations (19) and (23)–(27), is given by:

$$\mathbf{Z}_{x=L} = \mathbf{G} \mathbf{H} \quad (31)$$

where

$$\mathbf{z}_{x=L} = \begin{Bmatrix} U \\ W \\ \Phi \\ F \\ M \\ V \end{Bmatrix}_{x=L}, \mathbf{G} = \begin{bmatrix} G_{11} & G_{12} & G_{13} & G_{14} & G_{15} & G_{16} \\ G_{21} & G_{22} & G_{23} & G_{24} & G_{25} & G_{26} \\ G_{31} & G_{32} & G_{33} & G_{34} & G_{35} & G_{36} \\ G_{41} & G_{42} & G_{43} & G_{44} & G_{45} & G_{46} \\ G_{51} & G_{52} & G_{53} & G_{54} & G_{55} & G_{56} \\ G_{61} & G_{62} & G_{63} & G_{64} & G_{65} & G_{66} \end{bmatrix}, \quad (32)$$

and $G_{1j} = e^{\lambda_j L}, G_{2j} = \beta_j e^{\lambda_j L}, G_{3j} = \lambda_j \beta_j e^{\lambda_j L}, G_{4j} = -2E_f A_f \lambda_j e^{\lambda_j L},$

$$G_{5j} = -2E_f I_f \beta_j \lambda_j^2 e^{\lambda_j L}, G_{6j} = E_f I_f \left\{ 2\lambda_j^3 \beta_j - \frac{a^2 c}{r^2} (c\lambda_j \beta_j + 2) \right\} e^{\lambda_j L}.$$

By substituting Equation (30) into Equation (31), the relationship between state vectors $\mathbf{Z}_{x=0}$ and $\mathbf{Z}_{x=L}$ can be expressed as follows:

$$\mathbf{Z}_{x=L} = \mathbf{T} \mathbf{Z}_{x=0}, \quad (33)$$

where $\mathbf{T} = \mathbf{G} \mathbf{C}^{-1}$, and \mathbf{T} is the transfer matrix of the three-layered beam element.

From Equation (33), the natural frequencies and mode shapes of the three-layered beams with classical boundary conditions can be computed by determining the frequency determinant of the transfer matrix [31]. The end conditions of the displacements and forces used for applying the boundary condition to Equation (33) are $U, W, \Phi = 0$ and $F, M, V \neq 0$ at the clamped end and $U, W, \Phi \neq 0$ and $F, M, V = 0$ at the free end. In addition, the conditions $U, W, M = 0$ and $\Phi, V, F \neq 0$ are applied at the pinned end.

3. Results and Discussions

To demonstrate the accuracy of the developed method, the natural frequencies computed using the developed transfer matrix method were compared with the natural frequencies discussed in previous works. MATLAB(R2021b) was used to compute the results. The C-F end condition was investigated, and the results are listed in Table 1. The parameters of the sandwich beam used to predict the results shown in Table 1 are as follows [26,27]: $E_f A_f = 31,500 \text{ N}, E_f I_f = 1.362 \text{ Nm}^2, k_c A_c G_c = 1050 \text{ N}, m_f = 0.001225 \text{ kg/m}, h_f = 0.4527 \text{ mm}, h_c = 12.7 \text{ mm}, L = 0.9144 \text{ m}.$ The results of the present study and previous studies showed

excellent agreement. Because there were no results for the C-C, C-P, and P-P end conditions in previous studies, they are listed in Table 2 to analyze the effects of the axial and bending modes, for example, beams with various end conditions.

Table 1. Comparison of the results of previous studies and the present method for the first four natural frequencies of a symmetric three-layered beam with the cantilevered end condition.

ω_i	Natural Frequency [Hz]		
	Present	Banerjee [26]	Ruta and Szybiński [27]
1	31.459	31.46	31.46
2	193.71	193.7	193.7
3	529.20	529.2	529.2
4	1006.4	1006	1006

Table 2. First five natural frequencies of a symmetric three-layered beam with the different end conditions.

ω_i	Natural Frequency [Hz]			
	C-F	C-P	C-C	P-P
1	31.459	179.65	194.91	166.18
2	193.71	481.22	521.79	445.12
3	529.2	918.52	991.81	852.16
4	1006.4	1481.7	1590.1	1381.5
5	1612.8	2165.4	2308.9	2030.7

To analyze the dominant frequencies caused by the coupling of the axial and bending displacements for each boundary condition, the first five mode shapes of a sample beam structure with four classical end conditions are illustrated in Figure 2. As shown in Figure 2, the first five modes of this structure for all boundary conditions were dominated by bending frequencies, as expected. Because the length-to-height ratio (L/h) of a three-layered beam is very large (67.21), all modes appear to be dominated by the bending frequencies.

To investigate the effect of the axial modes, the variation in the first five natural frequencies was examined by changing the length-to-height ratio from 10 to 70 in steps of 10. The results are tabulated in Table 3, and the first five mode shapes of the three-layered beams for $L/h = 10$ are shown in Figure 3. As shown in Figure 3, the third and fifth mode shapes in the C-P, C-C, and P-P end conditions are clearly shown to dominate the axial frequencies, whereas the third and fourth mode shapes in the C-F end condition appear to be strongly influenced by both the axial and bending modes. This is caused by the coupling of the axial and bending displacements.

For a more detailed investigation of this phenomenon, an effective method capable of distinguishing the effects of strain energy is proposed. From Equations (1), (2) and (4), the maximum strain and kinetic energies can be defined as follows:

$$U_{max} = \int_0^L \left\{ E_f A_f \left(\frac{dU(x)}{dx} \right)^2 + E_f I_f \left(\frac{d^2W(x)}{dx^2} \right)^2 + \frac{1}{2} k_c A_c G_c \left(\frac{2}{h_c} U(x) + \left(1 + \frac{h_f}{h_c} \right) \frac{dW(x)}{dx} \right)^2 \right\} dx \quad (34)$$

$$T_{max} = \omega^2 \int_0^L m_f \{ (U(x))^2 + (W(x))^2 \} dx \quad (35)$$

By equating the maximum strain energy (U_{max}) and maximum kinetic energy (T_{max}), the following equation is obtained:

$$\omega^2 = S_f (= S_{f,a} + S_{f,b}) + S_c \quad (36)$$

where S_f is the effect of the face strain energy on the natural frequency, and $S_{f,a}$ and $S_{f,b}$ are the axial and bending strain energies, respectively.

$$S_f = S_{f,a} + S_{f,b} = \sum_{i=0}^n \frac{E_f A_f \left(\frac{dU(x_i)}{dx}\right)^2}{m_f \left\{ (U(x_i))^2 + (W(x_i))^2 \right\}} + \sum_{i=0}^n \frac{E_f I_f \left(\frac{d^2W(x_i)}{dx^2}\right)^2}{m_f \left\{ (U(x_i))^2 + (W(x_i))^2 \right\}} \quad (37)$$

and S_c is the effect of the core strain energy on the natural frequency,

$$S_c = \sum_{i=0}^n \frac{\frac{1}{2} k_c A_c G_c \left\{ \frac{2}{h_c} U(x_i) + \left(1 + \frac{h_f}{h_c}\right) \frac{dW(x_i)}{dx} \right\}^2}{m_f \left\{ (U(x_i))^2 + (W(x_i))^2 \right\}} \quad (38)$$

Therefore, the effect of the strain energies of the core and faces can be deduced from Equation (36):

$$C_f (= C_{f,a} + C_{f,b}) + C_c = 1 \quad (39)$$

where $C_f (= S_f / \omega^2)$ is the effect of the normal strain energy of the face layers on the natural frequency of free vibrations of a symmetric three-layered beam, and $C_c (= S_c / \omega^2)$ is the effect of the strain energy of the core layer. In addition, $C_{f,a} (= S_{f,a} / \omega^2)$ and $C_{f,b} (= S_{f,b} / \omega^2)$ are the effects of the axial and bending strain energies in the face layer, respectively.

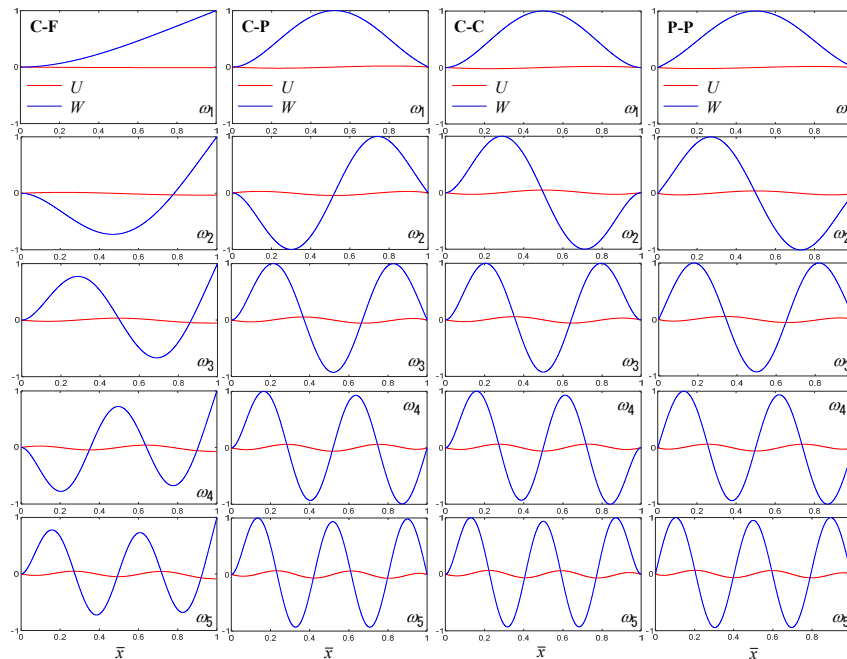


Figure 2. First five mode shapes of the symmetric three-layered beam with four classical end conditions.

By using Equation (39), the effects of the axial, bending, and shear strain energies on the natural frequencies can be analyzed. The effect of variations in these strain energies on the natural frequencies of three-layered beams with four end conditions are presented in Tables 4–11. TMM and Equation (36), as shown in Tables 4–11, are the natural frequencies computed using the transfer matrix method and Equation (36), respectively. The effect of the strain energies on the first natural frequency of three-layered beams with different end conditions, depending on the variation in L/h , is presented in Table 4. The effects of the strain energies on the natural frequencies of the three-layered beams with the C-F end condition, depending on the variation in L/h , are listed in Tables 5 and 6. The effects of the strain energies on the natural frequencies of the three-layered beams with the C-P end

condition, depending on the variation in L/h , are listed in Tables 7 and 8. The effects of the strain energy on the natural frequencies of the three-layered beams with the C-C end condition, depending on the variation in L/h , are summarized in Tables 9 and 10. Further, the effects of the strain energies on the natural frequencies of the three-layered beams with the P-P end condition, depending on the variation in L/h , are presented in Tables 11 and 12.

Table 3. Effects of the variation of L/h on the first five natural frequencies of the symmetric three-layered beam with the classical boundary conditions.

BCs	ω_i	Natural Frequency [Hz]						
		$L/h = 10$	$L/h = 20$	$L/h = 30$	$L/h = 40$	$L/h = 50$	$L/h = 60$	$L/h = 70$
C-F	1	1310.27	345.99	156.09	88.332	56.700	39.441	28.964
	2	7011.14	1954.89	917.34	530.69	345.03	241.91	179.11
	3	18,088.83	5089.99	2413.49	1415.47	930.62	657.89	489.23
	4	19,682.60	9470.86	4480.32	2642.07	1749.99	1245.75	931.88
	5	32,498.4	15,123.1	7119.82	4192.78	2784.40	1990.21	1495.33
C-C	1	6897.36	1911.31	905.78	528.24	345.30	242.96	180.05
	2	18,331.8	4940.14	2342.93	1380.56	911.99	647.23	482.80
	3	24,893.4	9342.52	4390.35	2588.27	1717.59	1225.63	918.96
	4	35,425.9	15,090.0	7023.93	4126.09	2739.84	1960.30	1474.85
	5	40,805.0	18,899.5	10,253.1	5992.01	3971.80	2843.09	2142.57
P-P	1	3665.73	1230.82	652.27	407.94	279.50	203.35	154.50
	2	12,209.0	3508.24	1762.27	1087.04	744.22	543.14	414.15
	3	24,878.8	7170.46	3469.72	2100.78	1427.38	1039.58	793.18
	4	26,431.7	12,201.3	5775.96	3448.74	2325.13	1687.17	1285.73
	5	40,779.7	18,616.8	8683.41	5130.46	3436.08	2483.81	1889.17
C-P	1	5071.04	1526.65	764.63	462.35	309.75	221.79	166.58
	2	15,090.2	4174.85	2031.11	1223.08	822.37	591.93	446.57
	3	24,880.3	8208.9	3908.08	2332.14	1564.95	1127.86	853.09
	4	30,755.4	13600.2	6378.66	3775.09	2524.52	1818.33	1376.53
	5	40,783.5	18,896.6	9447.37	5549.20	3696.06	2657.91	2011.81

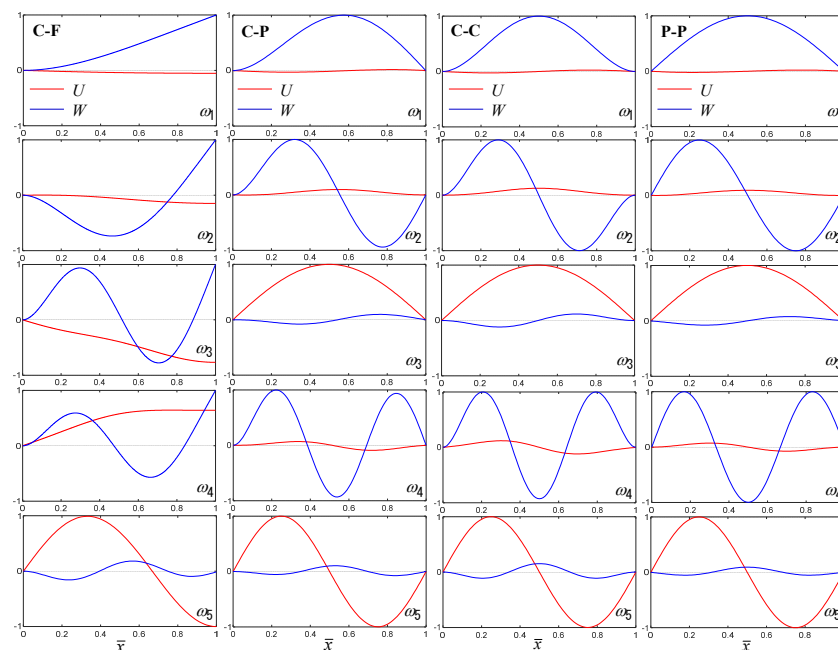


Figure 3. First five mode shapes of the symmetric three-layered beam with four end conditions when $L/h = 10$.

Table 4. Effect of strain energies on the first natural frequency of three-layered beams with different end conditions depending on the variation in L/h .

BCs.		Effect of Strain Energy on the First Natural Frequency [Hz]						
		$L/h = 10$	$L/h = 20$	$L/h = 30$	$L/h = 40$	$L/h = 50$	$L/h = 60$	$L/h = 70$
C-F	TMM	1310.3	345.99	156.09	88.332	56.700	39.441	29.007
	$C_{f,a}$	0.2977	0.4212	0.4596	0.4757	0.4839	0.4886	0.4915
	$C_{f,b}$	0.5954	0.5317	0.5152	0.5088	0.5057	0.5040	0.5029
	C_c	0.1068	0.0471	0.0252	0.0155	0.0104	0.0074	0.0056
	Equation (36)	1310.3	345.99	156.09	88.332	56.700	39.441	29.007
C-P	TMM	5071.0	1526.7	764.63	462.35	309.75	221.79	166.50
	$C_{f,a}$	0.0331	0.1636	0.2877	0.3709	0.4230	0.4557	0.4768
	$C_{f,b}$	0.7606	0.5332	0.4388	0.4041	0.3935	0.3927	0.3960
	C_c	0.2063	0.3032	0.2736	0.2250	0.1835	0.1515	0.1273
	Equation (36)	5071.1	1526.7	764.65	462.36	309.76	221.80	166.50
C-C	TMM	6897.4	1911.3	905.78	528.24	345.30	242.96	180.05
	$C_{f,a}$	0.0231	0.1288	0.2386	0.3155	0.3658	0.3991	0.4218
	$C_{f,b}$	0.8646	0.7048	0.6206	0.5773	0.5532	0.5386	0.5292
	C_c	0.1123	0.1664	0.1409	0.1072	0.0810	0.0623	0.0490
	Equation (36)	6897.5	1911.3	905.8	528.2	345.3	243.0	180.1
P-P	TMM	3665.7	1230.8	652.27	407.94	279.50	203.34	154.46
	$C_{f,a}$	0.0493	0.2104	0.3449	0.4300	0.4813	0.5121	0.5308
	$C_{f,b}$	0.5957	0.3350	0.2548	0.2370	0.2419	0.2547	0.2698
	C_c	0.3550	0.4545	0.4004	0.3330	0.2769	0.2332	0.1994
	Equation (36)	3665.8	1230.8	652.28	407.95	279.51	203.35	154.47

Table 5. Effect of strain energies on the natural frequencies of three-layered beams with the C-F end condition depending on the variation in L/h .

ω_i		Effect of Strain Energy on the Natural Frequency [Hz]							
		$L/h = 10$	$L/h = 12$	$L/h = 14$	$L/h = 16$	$L/h = 18$	$L/h = 20$	$L/h = 22$	$L/h = 24$
1	TMM	1310.3	927.19	690.32	533.69	424.77	345.99	287.20	242.18
	$C_{f,a}$	0.2977	0.3376	0.3673	0.3899	0.4074	0.4212	0.4322	0.4411
	$C_{f,b}$	0.5954	0.5732	0.5577	0.5464	0.5381	0.5317	0.5268	0.5229
	C_c	0.1068	0.0892	0.0750	0.0637	0.0545	0.0471	0.0410	0.0360
	Equation (36)	1310.3	927.19	690.32	533.69	424.77	345.99	287.20	242.18
2	TMM	7011.1	5007.1	3770.3	2949.5	2374.5	1954.9	1638.5	1393.8
	$C_{f,a}$	0.0867	0.1079	0.1325	0.1582	0.1837	0.2082	0.2313	0.2527
	$C_{f,b}$	0.7919	0.7553	0.7229	0.6950	0.6712	0.6508	0.6335	0.6187
	C_c	0.1214	0.1368	0.1445	0.1468	0.1451	0.1410	0.1352	0.1286
	Equation (36)	7011.1	5007.1	3770.3	2949.5	2374.5	1954.9	1638.5	1393.8
3	TMM	18,088.8	13,139.1	9855.2	7688.2	6182.0	5090.0	4270.9	3639.4
	$C_{f,a}$	0.1203	0.0471	0.0571	0.0716	0.0879	0.1052	0.1228	0.1406
	$C_{f,b}$	0.5728	0.8471	0.8246	0.7978	0.7722	0.7486	0.7273	0.7080
	C_c	0.3069	0.1058	0.1182	0.1306	0.1399	0.1462	0.1499	0.1514
	Equation (36)	18,088.8	13,139.1	9855.2	7688.2	6182.0	5090.0	4270.9	3639.4
4	TMM	19,682.6	18,301.7	17,350.3	14,312.3	11,520.0	9470.9	7935.7	6756.0
	$C_{f,a}$	0.1431	0.1705	0.1112	0.0383	0.0418	0.0506	0.0612	0.0729
	$C_{f,b}$	0.3275	0.0389	0.2809	0.8350	0.8412	0.8240	0.8046	0.7854
	C_c	0.5294	0.7906	0.6079	0.1267	0.1171	0.1254	0.1342	0.1417
	Equation (36)	19,682.6	18,301.7	17,350.3	14,312.3	11,520.0	9470.9	7935.7	6756.0

Table 5. Cont.

ω_i		Effect of Strain Energy on the Natural Frequency [Hz]							
		$L/h = 10$	$L/h = 12$	$L/h = 14$	$L/h = 16$	$L/h = 18$	$L/h = 20$	$L/h = 22$	$L/h = 24$
5	TMM	32,498.4	25,214.5	19,198.6	17,669.0	17,189.2	15,123.1	12,680.9	10,779.4
	$C_{f,a}$	0.7235	0.0258	0.0488	0.1008	0.0806	0.0354	0.0372	0.0430
	$C_{f,b}$	0.0161	0.8850	0.6222	0.0539	0.1269	0.8354	0.8515	0.8390
	C_c	0.2604	0.0892	0.3289	0.8453	0.7926	0.1292	0.1112	0.1181
	Equation (36)	32,498.4	25,214.5	19,198.6	17,669.0	17,189.2	15,123.1	12,680.9	10,779.4

Table 6. Effect of strain energies on the natural frequencies of three-layered beams with the C-F end condition depending on the variation in L/h .

ω_i		Effect of Strain Energy on the Natural Frequency [Hz]							
		$L/h = 26$	$L/h = 28$	$L/h = 30$	$L/h = 40$	$L/h = 50$	$L/h = 60$	$L/h = 70$	
1	TMM	206.94	178.85	156.09	88.332	56.700	39.441	29.007	
	$C_{f,a}$	0.4484	0.4545	0.4596	0.4757	0.4839	0.4886	0.4915	
	$C_{f,b}$	0.5198	0.5173	0.5152	0.5088	0.5057	0.5040	0.5029	
	C_c	0.0318	0.0282	0.0252	0.0155	0.0104	0.0074	0.0056	
	Equation (36)	206.94	178.85	156.09	88.332	56.700	39.441	29.007	
2	TMM	1200.3	1044.6	917.336	530.686	345.033	241.909	178.831	
	$C_{f,a}$	0.2724	0.2904	0.3067	0.3682	0.4061	0.4304	0.4465	
	$C_{f,b}$	0.6060	0.5950	0.5856	0.5537	0.5364	0.5262	0.5197	
	C_c	0.1217	0.1146	0.1077	0.0781	0.0575	0.0435	0.0338	
	Equation (36)	1200.3	1044.6	917.336	530.686	345.033	241.909	178.831	
3	TMM	3141.3	2740.7	2413.5	1415.5	930.618	657.894	489.296	
	$C_{f,a}$	0.1581	0.1753	0.1918	0.2644	0.3189	0.3586	0.3876	
	$C_{f,b}$	0.6906	0.6750	0.6610	0.6091	0.5776	0.5574	0.5440	
	C_c	0.1513	0.1497	0.1472	0.1265	0.1036	0.0840	0.0684	
	Equation (36)	3141.3	2740.7	2413.5	1415.5	930.618	657.894	489.296	
4	TMM	5828.8	5085.8	4480.3	2642.1	1750.0	1245.7	931.908	
	$C_{f,a}$	0.0853	0.0982	0.1114	0.1770	0.2351	0.2829	0.3210	
	$C_{f,b}$	0.7672	0.7500	0.7339	0.6696	0.6260	0.5962	0.5753	
	C_c	0.1475	0.1518	0.1546	0.1535	0.1389	0.1209	0.1037	
	Equation (36)	5828.8	5085.8	4480.3	2642.1	1750.0	1245.7	931.908	
5	TMM	9285.2	8090.5	7119.8	4192.8	2784.4	1990.2	1495.2	
	$C_{f,a}$	0.0502	0.0583	0.0671	0.1171	0.1690	0.2168	0.2583	
	$C_{f,b}$	0.8236	0.8079	0.7926	0.7252	0.6746	0.6374	0.6100	
	C_c	0.1262	0.1338	0.1403	0.1576	0.1564	0.1458	0.1317	
	Equation (36)	9285.2	8090.5	7119.8	4192.8	2784.4	1990.2	1495.2	

Table 7. Effect of strain energies on the natural frequencies of three-layered beams with the C-P end condition depending on the variation in L/h .

ω_i		Effect of Strain Energy on the Natural Frequency [Hz]							
		$L/h = 10$	$L/h = 12$	$L/h = 14$	$L/h = 16$	$L/h = 18$	$L/h = 20$	$L/h = 22$	$L/h = 24$
1	TMM	5071.0	3670.0	2806.4	2231.2	1825.6	1526.7	1298.8	1120.3
	$C_{f,a}$	0.0331	0.0542	0.0792	0.1066	0.1351	0.1636	0.1913	0.2179
	$C_{f,b}$	0.7606	0.7013	0.6488	0.6036	0.5653	0.5332	0.5065	0.4844
	C_c	0.2063	0.2444	0.2720	0.2898	0.2997	0.3032	0.3022	0.2977
	Equation (36)	5071.1	3670.0	2806.4	2231.3	1825.6	1526.7	1298.8	1120.4

Table 7. Cont.

ω_i		Effect of Strain Energy on the Natural Frequency [Hz]							
		$L/h = 10$	$L/h = 12$	$L/h = 14$	$L/h = 16$	$L/h = 18$	$L/h = 20$	$L/h = 22$	$L/h = 24$
2	TMM	15,090.2	10,684.9	8010.9	6261.4	5050.5	4174.9	3519.1	3013.7
	$C_{f,a}$	0.0181	0.0234	0.0320	0.0428	0.0554	0.0695	0.0847	0.1007
	$C_{f,b}$	0.8946	0.8623	0.8287	0.7956	0.7637	0.7336	0.7055	0.6795
	C_c	0.0873	0.1143	0.1393	0.1616	0.1809	0.1969	0.2098	0.2197
	Equation (36)	15,090.4	10,685.0	8011.0	6261.5	5050.6	4174.9	3519.1	3013.7
3	TMM	24,880.3	21,606.4	16,076.4	12,473.7	9992.9	8208.9	6880.8	5863.6
	$C_{f,a}$	0.5572	0.0132	0.0162	0.0217	0.0286	0.0366	0.0457	0.0557
	$C_{f,b}$	0.0025	0.9173	0.8964	0.8729	0.8492	0.8256	0.8026	0.7804
	C_c	0.4403	0.0696	0.0874	0.1053	0.1222	0.1377	0.1517	0.1639
	Equation (36)	24,880.4	21,606.6	16,076.5	12,473.8	9993.0	8209.0	6880.9	5863.7
4	TMM	30,755.4	22,629.6	21,151.4	20,078.0	16,612.5	13,600.2	11,360.1	9649.0
	$C_{f,a}$	0.0112	0.4678	0.3941	0.3087	0.0177	0.0205	0.0256	0.0316
	$C_{f,b}$	0.9386	0.0031	0.0028	0.0823	0.8930	0.8785	0.8606	0.8425
	C_c	0.0502	0.5290	0.6032	0.6090	0.0893	0.1010	0.1138	0.1259
	Equation (36)	30,755.7	22,629.7	21,151.5	20,078.1	16,612.7	13,600.3	11,360.2	9649.1
5	TMM	40,783.5	35,173.8	26,984.4	20,914.1	19,442.0	18,896.6	16,975.3	14,383.7
	$C_{f,a}$	0.8300	0.7760	0.0092	0.0361	0.2809	0.2421	0.0165	0.0197
	$C_{f,b}$	0.0030	0.0020	0.9298	0.8333	0.0048	0.0015	0.8970	0.8828
	C_c	0.1669	0.2220	0.0611	0.1307	0.7142	0.7564	0.0865	0.0975
	Equation (36)	40,783.8	35,174.1	26,984.7	20,914.3	19,442.1	18,896.7	16,975.5	14,383.8

Table 8. Effect of strain energies on the natural frequencies of three-layered beams with the C-P end condition depending on the variation in L/h .

ω_i		Effect of Strain Energy on the Natural Frequency [Hz]						
		$L/h = 26$	$L/h = 28$	$L/h = 30$	$L/h = 40$	$L/h = 50$	$L/h = 60$	$L/h = 70$
1	TMM	977.48	861.01	764.63	462.35	309.75	221.79	166.50
	$C_{f,a}$	0.2429	0.2661	0.2877	0.3709	0.4230	0.4557	0.4768
	$C_{f,b}$	0.4661	0.4511	0.4388	0.4041	0.3935	0.3927	0.3960
	C_c	0.2910	0.2828	0.2736	0.2250	0.1835	0.1515	0.1273
	Equation (36)	977.50	861.03	764.65	462.36	309.76	221.80	166.50
2	TMM	2614.9	2293.9	2031.1	1223.1	822.37	591.93	446.57
	$C_{f,a}$	0.1173	0.1341	0.1510	0.2306	0.2959	0.3460	0.3835
	$C_{f,b}$	0.6557	0.6340	0.6142	0.5405	0.4972	0.4721	0.4577
	C_c	0.2270	0.2319	0.2348	0.2289	0.2070	0.1819	0.1587
	Equation (36)	2614.9	2293.9	2031.1	1223.1	822.38	591.94	446.58
3	TMM	5065.9	4427.6	3908.1	2332.1	1565.0	1127.9	853.01
	$C_{f,a}$	0.0664	0.0777	0.0894	0.1508	0.2097	0.2613	0.3045
	$C_{f,b}$	0.7591	0.7389	0.7197	0.6401	0.5840	0.5451	0.5185
	C_c	0.1745	0.1835	0.1909	0.2091	0.2063	0.1935	0.1770
	Equation (36)	5066.0	4427.7	3908.1	2332.2	1565.0	1127.9	853.03
4	TMM	8311.2	7244.2	6378.7	3775.1	2524.5	1818.3	1376.5
	$C_{f,a}$	0.0384	0.0458	0.0539	0.0998	0.1492	0.1967	0.2396
	$C_{f,b}$	0.8245	0.8069	0.7897	0.7135	0.6538	0.6086	0.5746
	C_c	0.1371	0.1473	0.1564	0.1867	0.1969	0.1947	0.1858
	Equation (36)	8311.2	7244.3	6378.7	3775.1	2524.6	1818.4	1376.5

Table 8. Cont.

ω_i		Effect of Strain Energy on the Natural Frequency [Hz]						
		$L/h = 26$	$L/h = 28$	$L/h = 30$	$L/h = 40$	$L/h = 50$	$L/h = 60$	$L/h = 70$
5	TMM	12,360.9	10,750.8	9447.4	5549.2	3696.1	2657.9	2011.8
	$C_{f,a}$	0.0238	0.0286	0.0339	0.0670	0.1066	0.1480	0.1878
	$C_{f,b}$	0.8680	0.8531	0.8384	0.7687	0.7098	0.6621	0.6242
	C_c	0.1082	0.1183	0.1278	0.1643	0.1836	0.1900	0.1880
	Equation (36)	12,361.0	10,750.9	9447.5	5549.3	3696.1	2657.9	2011.9

Table 9. Effect of strain energies on the natural frequencies of three-layered beams with the C-C end condition depending on the variation in L/h .

ω_i		Effect of Strain Energy on the Natural Frequency [Hz]							
		$L/h = 10$	$L/h = 12$	$L/h = 14$	$L/h = 16$	$L/h = 18$	$L/h = 20$	$L/h = 22$	$L/h = 24$
1	TMM	6897.4	4899.8	3680.6	2877.8	2318.3	1911.3	1604.9	1367.9
	$C_{f,a}$	0.0231	0.0390	0.0586	0.0808	0.1045	0.1288	0.1528	0.1761
	$C_{f,b}$	0.8646	0.8264	0.7907	0.7585	0.7299	0.7048	0.6830	0.6640
	C_c	0.1123	0.1346	0.1506	0.1607	0.1656	0.1664	0.1642	0.1599
	Equation (36)	6897.5	4899.9	3680.7	2877.8	2318.4	1911.3	1604.9	1367.9
2	TMM	18,331.8	12,919.2	9635.2	7490.3	6008.8	4940.1	4141.9	3528.6
	$C_{f,a}$	0.0186	0.0195	0.0259	0.0349	0.0458	0.0584	0.0722	0.0869
	$C_{f,b}$	0.9190	0.8979	0.8727	0.8472	0.8224	0.7987	0.7764	0.7556
	C_c	0.0624	0.0826	0.1014	0.1179	0.1318	0.1430	0.1515	0.1575
	Equation (36)	18,332.1	12,919.5	9635.4	7490.4	6008.9	4940.2	4142.0	3528.6
3	TMM	24,893.4	22,629.1	18,440.1	14,271.2	11,402.9	9342.5	7810.4	6638.3
	$C_{f,a}$	0.5540	0.4684	0.0138	0.0181	0.0239	0.0309	0.0389	0.0479
	$C_{f,b}$	0.0060	0.0020	0.9164	0.8972	0.8775	0.8577	0.8383	0.8195
	C_c	0.4400	0.5296	0.0698	0.0847	0.0986	0.1114	0.1228	0.1326
	Equation (36)	24,893.5	22,629.2	18,440.4	14,271.4	11,403.1	9342.7	7810.5	6638.4
4	TMM	35,425.9	24,844.3	21,152.3	20,127.3	18,429.4	15,090.0	12,586.6	10,674.5
	$C_{f,a}$	0.0179	0.0114	0.3943	0.3321	0.0295	0.0182	0.0221	0.0273
	$C_{f,b}$	0.9438	0.9342	0.0019	0.0075	0.8682	0.8953	0.8809	0.8653
	C_c	0.0382	0.0544	0.6037	0.6604	0.1022	0.0865	0.0969	0.1073
	Equation (36)	35,426.6	24,844.8	21,152.4	20,127.4	18,429.7	15,090.3	12,586.9	10,674.7
5	TMM	40,805.0	35,176.3	30,077.3	23,221.7	19,477.6	18,899.5	18,487.0	15,658.3
	$C_{f,a}$	0.8224	0.7756	0.0081	0.0113	0.2670	0.2416	0.2090	0.0177
	$C_{f,b}$	0.0098	0.0022	0.9413	0.9213	0.0453	0.0026	0.0024	0.8970
	C_c	0.1678	0.2222	0.0506	0.0674	0.6876	0.7557	0.7887	0.0853
	Equation (36)	40,805.3	35,176.6	30,077.9	23,222.1	19,477.6	18,899.5	18,487.0	15,658.6

Table 10. Effect of strain energies on the natural frequencies of three-layered beams with the C-C end condition depending on the variation in L/h .

ω_i		Effect of Strain Energy on the Natural Frequency [Hz]						
		$L/h = 26$	$L/h = 28$	$L/h = 30$	$L/h = 40$	$L/h = 50$	$L/h = 60$	$L/h = 70$
1	TMM	1180.4	1029.4	905.78	528.24	345.30	242.96	180.05
	$C_{f,a}$	0.1983	0.2191	0.2386	0.3155	0.3658	0.3991	0.4218
	$C_{f,b}$	0.6475	0.6331	0.6206	0.5773	0.5532	0.5386	0.5292
	C_c	0.1543	0.1478	0.1409	0.1072	0.0810	0.0623	0.0490
	Equation (36)	1180.5	1029.4	905.8	528.2	345.3	243.0	180.1

Table 10. Cont.

ω_i		Effect of Strain Energy on the Natural Frequency [Hz]						
		$L/h = 26$	$L/h = 28$	$L/h = 30$	$L/h = 40$	$L/h = 50$	$L/h = 60$	$L/h = 70$
2	TMM	3046.1	2658.9	2342.9	1380.6	911.99	647.23	482.81
	$C_{f,a}$	0.1023	0.1180	0.1338	0.2087	0.2701	0.3172	0.3526
	$C_{f,b}$	0.7365	0.7189	0.7028	0.6412	0.6021	0.5766	0.5592
	C_c	0.1612	0.1631	0.1634	0.1501	0.1278	0.1063	0.0881
3	Equation (36)	3046.1	2658.9	2343.0	1380.6	912.01	647.24	482.82
	TMM	5720.2	4986.6	4390.3	2588.3	1717.6	1225.6	918.96
	$C_{f,a}$	0.0577	0.0681	0.0791	0.1381	0.1953	0.2452	0.2866
	$C_{f,b}$	0.8014	0.7841	0.7678	0.6997	0.6513	0.6172	0.5928
	C_c	0.1410	0.1477	0.1531	0.1623	0.1534	0.1376	0.1206
4	Equation (36)	5720.3	4986.7	4390.4	2588.3	1717.6	1225.6	918.98
	TMM	9180.2	7989.3	7023.9	4126.1	2739.8	1960.3	1474.8
	$C_{f,a}$	0.0334	0.0401	0.0475	0.0909	0.1390	0.1857	0.2278
	$C_{f,b}$	0.8496	0.8341	0.8190	0.7513	0.6984	0.6584	0.6282
	C_c	0.1170	0.1258	0.1335	0.1578	0.1625	0.1559	0.1440
5	Equation (36)	9180.4	7989.5	7024.1	4126.2	2739.9	1960.3	1474.8
	TMM	13,442.7	11,679.7	10,253.1	5992.0	3971.8	2843.1	2142.5
	$C_{f,a}$	0.0211	0.0253	0.0301	0.0608	0.0989	0.1394	0.1788
	$C_{f,b}$	0.8840	0.8708	0.8575	0.7946	0.7410	0.6977	0.6635
	C_c	0.0948	0.1039	0.1124	0.1446	0.1601	0.1629	0.1577
	Equation (36)	13,443.0	11,680.0	10,253.3	5992.1	3971.9	2843.1	2142.6

Table 11. Effect of strain energies on the natural frequencies of three-layered beams with the P-P end condition depending on the variation in L/h .

ω_i		Effect of Strain Energy on the Natural Frequency [Hz]							
		$L/h = 10$	$L/h = 12$	$L/h = 14$	$L/h = 16$	$L/h = 18$	$L/h = 20$	$L/h = 22$	$L/h = 24$
1	TMM	3665.7	2728.6	2138.8	1737.3	1448.2	1230.8	1062.0	927.61
	$C_{f,a}$	0.0493	0.0780	0.1102	0.1439	0.1777	0.2104	0.2415	0.2706
	$C_{f,b}$	0.5957	0.5187	0.4562	0.4062	0.3665	0.3350	0.3102	0.2907
	C_c	0.3550	0.4033	0.4336	0.4499	0.4558	0.4545	0.4482	0.4386
	Equation (36)	3665.8	2728.6	2138.8	1737.4	1448.2	1230.8	1062.1	927.63
2	TMM	12,209.0	8709.6	6580.6	5183.5	4212.9	3508.2	2978.1	2567.7
	$C_{f,a}$	0.0211	0.0290	0.0395	0.0521	0.0664	0.0822	0.0990	0.1166
	$C_{f,b}$	0.8544	0.8104	0.7667	0.7246	0.6851	0.6485	0.6150	0.5846
	C_c	0.1245	0.1606	0.1938	0.2233	0.2485	0.2693	0.2860	0.2988
	Equation (36)	12,209.1	8709.6	6580.6	5183.5	4213.0	3508.3	2978.2	2567.7
3	TMM	24,878.8	18,625.3	13,901.8	10,822.3	8699.2	7170.5	6030.6	5156.2
	$C_{f,a}$	0.5580	0.0142	0.0195	0.0262	0.0343	0.0435	0.0536	0.0645
	$C_{f,b}$	0.0014	0.8981	0.8702	0.8417	0.8132	0.7852	0.7581	0.7321
	C_c	0.4406	0.0877	0.1103	0.1321	0.1525	0.1713	0.1883	0.2033
	Equation (36)	24,878.9	18,625.3	13,901.8	10,822.3	8699.2	7170.5	6030.6	5156.2
4	TMM	26,431.7	22,628.7	21,146.2	18,596.2	14,879.9	12,201.3	10,210.3	8688.6
	$C_{f,a}$	0.0110	0.4687	0.3926	0.0213	0.0190	0.0237	0.0297	0.0365
	$C_{f,b}$	0.9241	0.0015	0.0071	0.8832	0.8770	0.8568	0.8359	0.8151
	C_c	0.0650	0.5298	0.6003	0.0954	0.1040	0.1194	0.1344	0.1484
	Equation (36)	26,431.7	22,628.8	21,146.3	18,596.2	14,880.0	12,201.3	10,210.3	8688.7

Table 11. Cont.

ω_i		Effect of Strain Energy on the Natural Frequency [Hz]							
		$L/h = 10$	$L/h = 12$	$L/h = 14$	$L/h = 16$	$L/h = 18$	$L/h = 20$	$L/h = 22$	$L/h = 24$
5	TMM	40,779.7	32,430.6	24,082.8	20,183.3	19,436.9	18,616.8	15,528.7	13,173.1
	$C_{f,a}$	0.8314	0.0081	0.0117	0.3253	0.2822	0.0153	0.0183	0.0223
	$C_{f,b}$	0.0018	0.9364	0.9121	0.0160	0.0015	0.8982	0.8824	0.8659
	C_c	0.1668	0.0555	0.0762	0.6587	0.7163	0.0865	0.0993	0.1118
	Equation (36)	40,780.0	32,430.6	24,082.8	20,183.4	19,436.9	18,616.8	15,528.7	13,173.1

Table 12. Effect of strain energies on the natural frequencies of three-layered beams with the P-P end condition depending on the variation in L/h .

ω_i		Effect of Strain Energy on the Natural Frequency [Hz]						
		$L/h = 26$	$L/h = 28$	$L/h = 30$	$L/h = 40$	$L/h = 50$	$L/h = 60$	$L/h = 70$
1	TMM	818.33	727.99	652.27	407.94	279.50	203.34	154.46
	$C_{f,a}$	0.2976	0.3223	0.3449	0.4300	0.4813	0.5121	0.5308
	$C_{f,b}$	0.2755	0.2637	0.2548	0.2370	0.2419	0.2547	0.2698
	C_c	0.4269	0.4140	0.4004	0.3330	0.2769	0.2332	0.1994
	Equation (36)	818.34	728.00	652.28	407.95	279.51	203.35	154.47
2	TMM	2242.2	1978.9	1762.3	1087.0	744.22	543.14	414.20
	$C_{f,a}$	0.1347	0.1530	0.1712	0.2561	0.3249	0.3772	0.4159
	$C_{f,b}$	0.5571	0.5325	0.5105	0.4318	0.3894	0.3679	0.3581
	C_c	0.3081	0.3145	0.3184	0.3121	0.2856	0.2549	0.2259
	Equation (36)	2242.3	1978.9	1762.3	1087.1	744.24	543.15	414.21
3	TMM	4469.3	3918.7	3469.7	2100.8	1427.4	1039.6	793.22
	$C_{f,a}$	0.0761	0.0881	0.1005	0.1646	0.2256	0.2792	0.3239
	$C_{f,b}$	0.7074	0.6841	0.6622	0.5723	0.5106	0.4694	0.4424
	C_c	0.2165	0.2278	0.2373	0.2631	0.2638	0.2515	0.2336
	Equation (36)	4469.3	3918.7	3469.7	2100.8	1427.4	1039.6	793.23
4	TMM	7498.0	6547.6	5776.0	3448.7	2325.1	1687.2	1285.7
	$C_{f,a}$	0.0441	0.0522	0.0609	0.1092	0.1600	0.2084	0.2523
	$C_{f,b}$	0.7946	0.7746	0.7553	0.6701	0.6041	0.5545	0.5178
	C_c	0.1613	0.1731	0.1838	0.2207	0.2359	0.2371	0.2299
	Equation (36)	7498.0	6547.7	5776.0	3448.8	2325.2	1687.2	1285.7
5	TMM	11,334.1	9869.6	8683.4	5130.5	3436.1	2483.8	1889.2
	$C_{f,a}$	0.0270	0.0323	0.0381	0.0736	0.1147	0.1568	0.1972
	$C_{f,b}$	0.8493	0.8326	0.8162	0.7394	0.6750	0.6230	0.5819
	C_c	0.1238	0.1351	0.1457	0.1870	0.2103	0.2202	0.2209
	Equation (36)	11,334.1	9869.6	8683.4	5130.5	3436.1	2483.8	1889.2

Based on the results computed in Tables 5–12, the effect of variations in the normal and shear strain energies on the natural frequencies of such beams, as well as the effect of change in axial, bending, and shear strain energies on the natural frequencies of three layered beams with different end conditions, are illustrated in Figures 4–7. In the dynamic behaviors of such beams, as shown in Figures 4–7, the bending modes for all boundary conditions are significantly affected by the normal strain energy of the face layer, but the effect of the shear strain energy of the core is also sufficiently large that it cannot be ignored. By observing the variations in the axial, bending, and shear strain energies represented in Figures 4–7, it can be concluded that the axial strain energy has a significant effect, even in the bending-dominated modes.

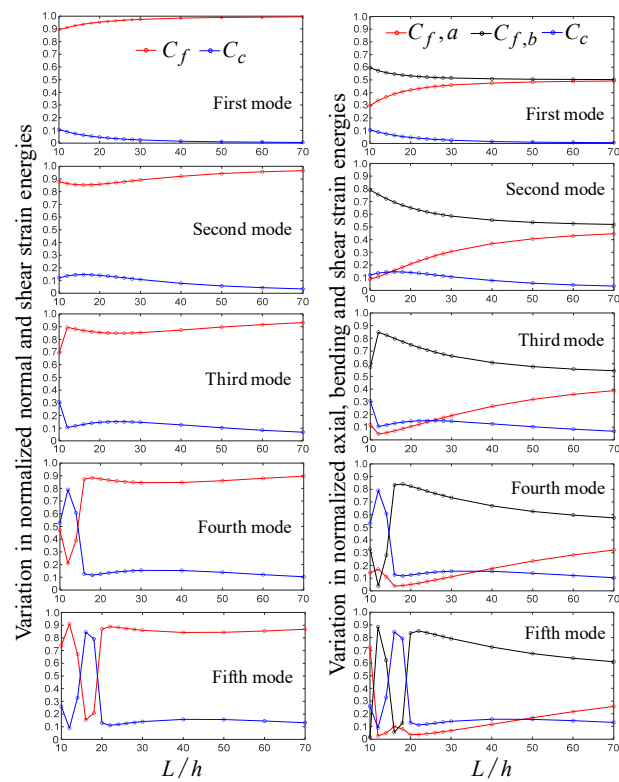


Figure 4. Variation in the strain energies on the natural frequencies of three-layered beams with the C-F end condition.

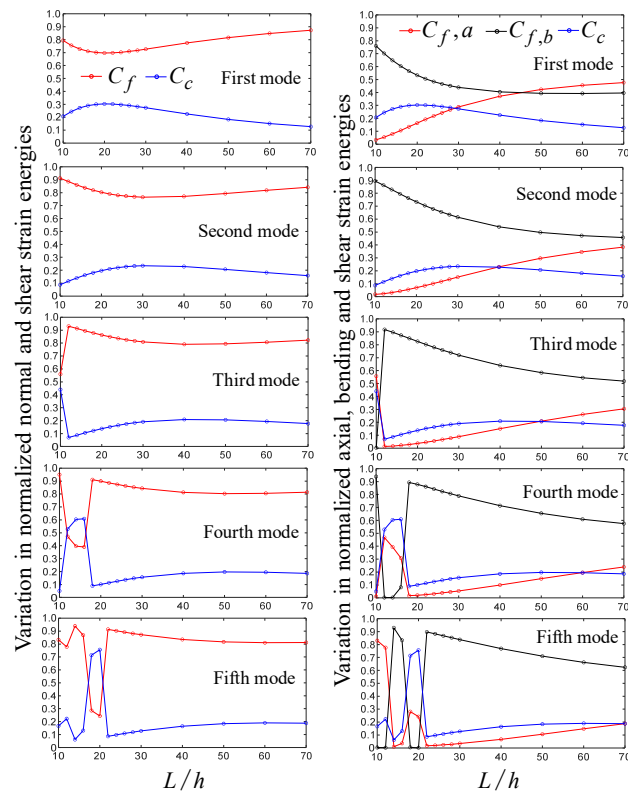


Figure 5. Variation in the strain energies on the natural frequencies of three-layered beams with the C-P end condition.

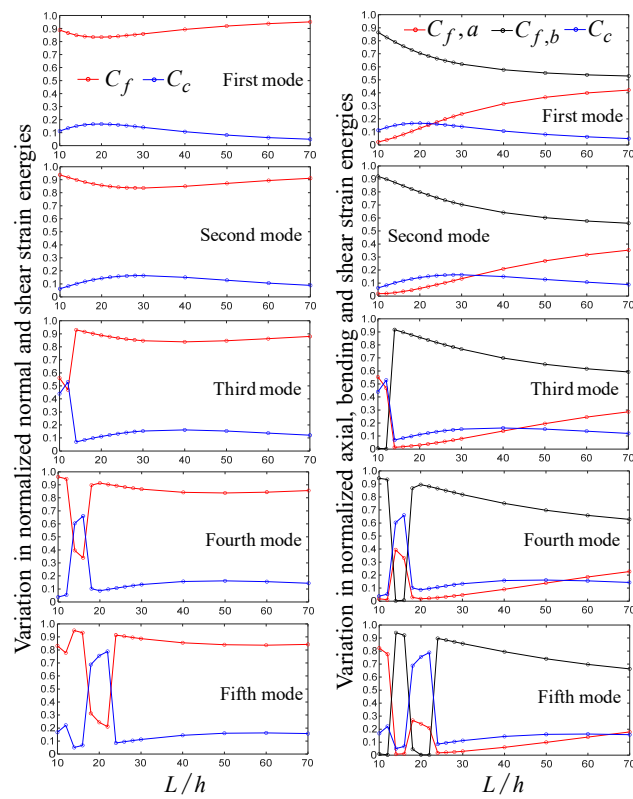


Figure 6. Variation in the strain energies on the natural frequencies of three-layered beams with the C-C end condition.

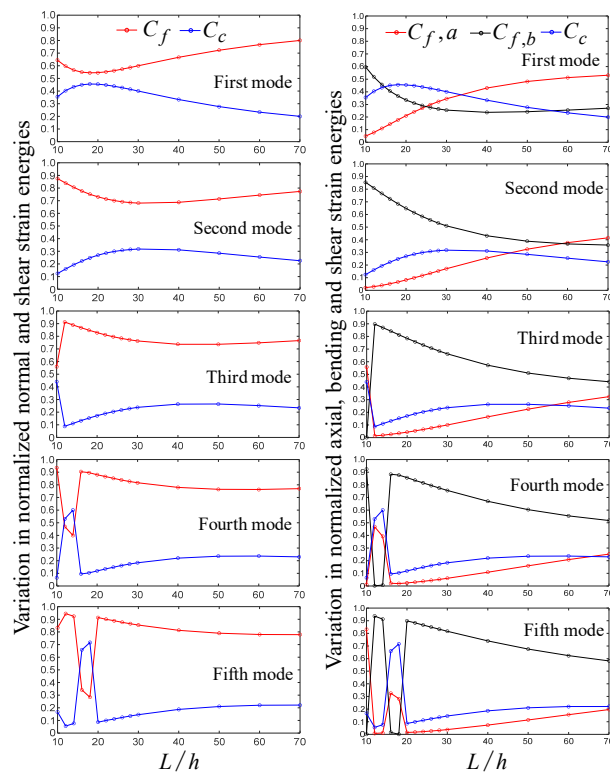


Figure 7. Variation in the strain energies on the natural frequencies of three-layered beams with the P-P end condition.

Moreover, all the strain energies in the fourth and fifth natural frequencies, as shown in Figures 4–7, undergo sudden changes. These phenomena can be analyzed in connection with the third and fourth mode shapes of the three-layered beam with the C-F end condition shown in Figure 3. To analyze the variation in mode shapes in detail, the variation in the mode shapes of three-layered beams with the cantilevered end condition, with respect to the change in L/h , was investigated. The mode shapes between $L/h = 10$ and $L/h = 20$ exhibited sudden changes in the strain energies. L/h was increased from 10 to 20 at intervals of 2, and the results are presented in Figure 8. As shown in Figure 8, the sudden changes in the axial, bending, and shear strain energies were found to be caused by the exchange process in the order of modes. In addition, it can be observed that the influence of the shear strain energy of the core is significantly increased in the exchange process in the order of the modes.

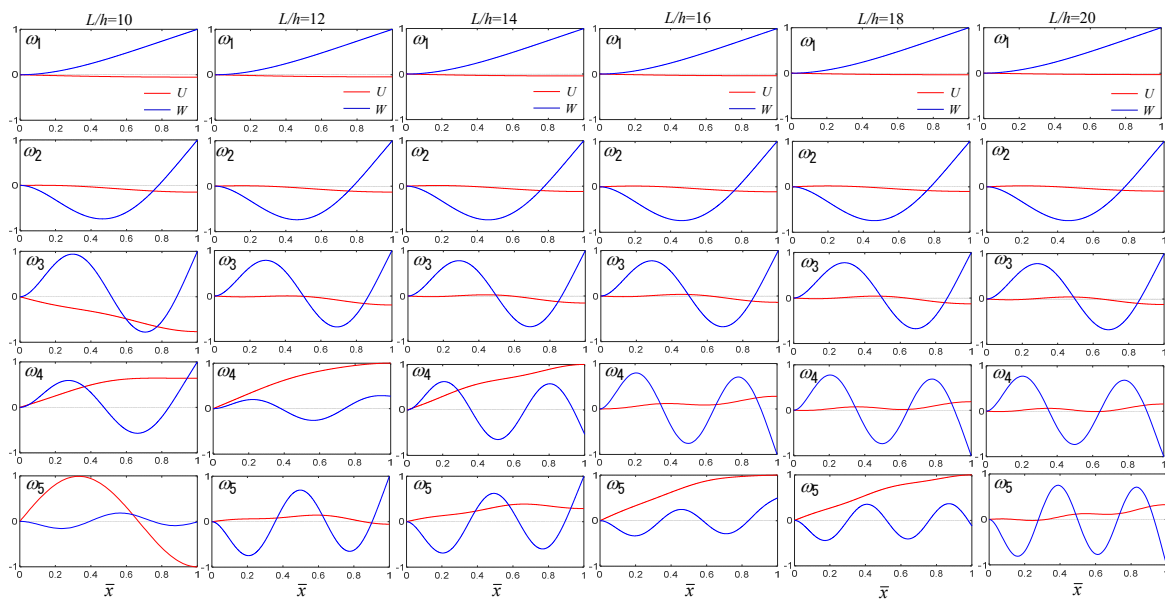


Figure 8. Variation in the first five mode shapes of soft-core three-layered beams with the cantilevered end condition with respect to the variation of L/h .

4. Conclusions

An analytical technique capable of distinguishing the effects of axial and bending displacements and shear deformation on the natural frequencies of three-layered beams was proposed in this study. The effect of these strain energies was calculated using the relation between the maximum normal strain and kinetic energies by applying the shape functions of the displacements defined by the developed transfer matrix. The transfer matrix method is used to determine the eigenpairs of three-layered beams with a soft core, and the efficacy of the method is demonstrated through a comparison of the results computed using the proposed method and those discussed in previous works.

From the analyzed results, all the bending-dominated modes of top and bottom layers were accompanied by the axial displacements because of the existence of a core layer, whereas the axial-dominated modes were uncoupled with the bending displacements. Moreover, the axial displacements have a significant effect, even in bending-dominated modes.

The proposed method has been considered a reasonable assumption for practical problems, but the method is somewhat limited for applications because the mass of the core layer was ignored, and the shear deformation beam theory was not considered in the top and bottom layers. For a wide range of applications for such beams, the mass and shear deformation in all layers should be considered in future studies.

Funding: This research was funded by the Kyonggi University grant number 2020.

Institutional Review Board Statement: Not applicable.

Informed Consent Statement: Not applicable.

Data Availability Statement: Not applicable.

Acknowledgments: This work was supported by the Kyonggi University Research Grant 2020.

Conflicts of Interest: The authors declare no conflict of interest.

References

1. Won, S.G.; Bae, S.H.; Cho, J.R.; Bae, S.R.; Jeong, W.B. Three-layered damped beam element for forced vibration analysis of symmetric sandwich structures with a viscoelastic core. *Finite Elem. Anal. Des.* **2013**, *68*, 39–51. [\[CrossRef\]](#)
2. Howson, W.P.; Zare, A. Exact dynamic stiffness matrix for flexural vibration of three-layered sandwich beams. *J. Sound Vib.* **2005**, *282*, 753–767. [\[CrossRef\]](#)
3. Asgari, G. Dynamic instability and free vibration behavior of three-layered soft-cored sandwich beams on nonlinear elastic foundations. *Struct. Eng. Mech. Int. J.* **2019**, *72*, 525–540.
4. Lv, H.W.; Li, L.; Li, Y.H. Non-linearly parametric resonances of an axially moving viscoelastic sandwich beam with time-dependent velocity. *Appl. Math. Model.* **2018**, *53*, 83–105. [\[CrossRef\]](#)
5. Park, M.J.; Yoon, S.W.; Ju, Y.K. New approaches for floor vibrations of steel–polymer–steel sandwich floor systems. *Eng. Struct.* **2022**, *258*, 114141. [\[CrossRef\]](#)
6. Jin, Y.; Yang, R.; Liu, H.; Xu, H.; Chen, H. A unified solution for the vibration analysis of lattice sandwich beams with general elastic supports. *Appl. Sci.* **2021**, *11*, 9141. [\[CrossRef\]](#)
7. Fadaee, M. A new reformulation of vibration suppression equations of functionally graded magnetorheological fluid sandwich beam. *Appl. Math. Model.* **2019**, *74*, 469–482. [\[CrossRef\]](#)
8. Li, Y.S.; Liu, B.L. Thermal buckling and free vibration of viscoelastic functionally graded sandwich shells with tunable auxetic honeycomb core. *Appl. Math. Model.* **2022**, *108*, 685–700. [\[CrossRef\]](#)
9. Bennai, R.; Ait Atmane, H.; Tounsi, A. A new higher-order shear and normal deformation theory for functionally graded sandwich beams. *Steel Compos. Struct.* **2015**, *19*, 521–546. [\[CrossRef\]](#)
10. Osofero, A.I.; Vo, T.P.; Nguyen, T.K.; Lee, J. Analytical solution for vibration and buckling of functionally graded sandwich beams using various quasi-3D theories. *J. Sandw. Struct. Mater.* **2016**, *18*, 3–29. [\[CrossRef\]](#)
11. Wang, P.; Wu, N.; Sun, Z.; Luo, H. Vibration and reliability analysis of non-uniform composite beam under random load. *Appl. Sci.* **2022**, *12*, 2700. [\[CrossRef\]](#)
12. Seyfi, A.; Teimouri, A.; Dimitri, R.; Tornabene, F. Dispersion of elastic waves in functionally graded CNTs-reinforced composite beams. *Appl. Sci.* **2022**, *12*, 3852. [\[CrossRef\]](#)
13. Chakrabarti, A.; Chalak, H.D.; Iqbal, M.A.; Sheikh, A.H. A new FE model based on higher order zigzag theory for the analysis of laminated sandwich beam with soft core. *Compos. Struct.* **2011**, *93*, 271–279. [\[CrossRef\]](#)
14. Damanpack, A.R.; Bodaghi, M. A new sandwich element for modeling of partially delaminated sandwich beam structures. *Compos. Struct.* **2021**, *256*, 113068. [\[CrossRef\]](#)
15. Sayyad, A.S.; Ghugal, Y.M. Bending, buckling and free vibration of laminated composite and sandwich beams: A critical review of literature. *Compos. Struct.* **2017**, *171*, 486–504. [\[CrossRef\]](#)
16. Garg, A.; Chalak, H.D. Novel higher-order zigzag theory for analysis of laminated sandwich beams. *Proc. Inst. Mech. Eng. Part L J. Mater. Des. Appl.* **2021**, *235*, 176–194. [\[CrossRef\]](#)
17. Wang, Y.; Wang, X. Free vibration analysis of soft-core sandwich beams by the novel weak form quadrature element method. *J. Sandw. Struct. Mater.* **2016**, *18*, 294–320. [\[CrossRef\]](#)
18. Gholami, M.; Alibazi, A.; Moradifard, R.; Deylughian, S. Out-of-plane free vibration analysis of three-layer sandwich beams using dynamic stiffness matrix. *Alex. Eng. J.* **2021**, *60*, 4981–4993. [\[CrossRef\]](#)
19. Khdeir, A.A.; Aldraihem, O.J. Free vibration of sandwich beams with soft core. *Compos. Struct.* **2016**, *154*, 179–189. [\[CrossRef\]](#)
20. Long, R.; Barry, O.; Oguamanam, D.C.D. Finite element free vibration analysis of soft-core sandwich beams. *AIAA J.* **2012**, *50*, 235–238. [\[CrossRef\]](#)
21. Chalak, H.D.; Chakrabarti, A.; Iqbal, M.A.; Sheikh, A.H. Vibration of laminated sandwich beams having soft core. *J. Vib. Control* **2012**, *18*, 1422–1435. [\[CrossRef\]](#)
22. Yang, X.D.; Zhang, W.; Chen, L.Q. Transverse vibrations and stability of axially traveling sandwich beam with soft core. *J. Vib. Acoust.* **2013**, *135*, 051013. [\[CrossRef\]](#)
23. Loja, M.A.R.; Barbosa, J.I.; Soares, C.M. Dynamic behaviour of soft core sandwich beam structures using kriging-based layerwise models. *Compos. Struct.* **2015**, *134*, 883–894. [\[CrossRef\]](#)
24. Sakiyama, T.; Matsuda, H.; Morita, C. Free vibration analysis of sandwich beam with elastic or viscoelastic core by applying the discrete Green function. *J. Sound Vib.* **1996**, *191*, 189–206. [\[CrossRef\]](#)
25. Ahmed, K. Free vibration of curved sandwich beams by the method of finite elements. *J. Sound Vib.* **1971**, *18*, 61–74. [\[CrossRef\]](#)
26. Banerjee, J.R. Free vibration of sandwich beams using the dynamic stiffness method. *Comput. Struct.* **2003**, *81*, 1915–1922. [\[CrossRef\]](#)
27. Ruta, P.; Szybiński, J. Free vibration of non-prismatic sandwich beams using the Chebyshev series. *Procedia Eng.* **2014**, *91*, 105–111. [\[CrossRef\]](#)

28. Yildirim, S. Free vibration analysis of sandwich beams with functionally-graded-cores by complementary functions method. *AIAA J.* **2020**, *58*, 5431–5439. [[CrossRef](#)]
29. Wang, J.T.; Wang, C.J.; Zhao, J.P. Frequency response function-based model updating using Kriging model. *Mech. Syst. Signal Process.* **2017**, *87*, 218–228. [[CrossRef](#)]
30. Sehgal, S.; Kumar, H. Development of efficient model updating technique using multi-stage response surfaces and derringer's function. In Proceedings of the 2014 Recent Advances in Engineering and Computational Sciences (RAECS), Chandigarh, India, 6–8 March 2014; pp. 1–6.
31. Wang, W.; Mottershead, J.E.; Ihle, A.; Siebert, T.; Schubach, H.R. Finite element model updating from full-field vibration measurement using digital image correlation. *J. Sound Vib.* **2011**, *330*, 1599–1620. [[CrossRef](#)]
32. Yildirim, V. Buckling analysis of rectangular beams having ceramic liners at its top and bottom surfaces with the help of the exact transfer matrix. *Int. J. Eng. Appl. Sci.* **2021**, *13*, 17–35. [[CrossRef](#)]
33. Bozdogan, K.B.; Ozturk, D. A method for static and dynamic analyses of stiffened multi-bay coupled shear walls. *Struct. Eng. Mech. Int. J.* **2008**, *28*, 479–489. [[CrossRef](#)]
34. Udayakumar, B.; Gopal, K.N. A modified state space differential quadrature method for free vibration analysis of soft-core sandwich panels. *J. Sandw. Struct. Mater.* **2019**, *21*, 1843–1879. [[CrossRef](#)]
35. Lee, J.W.; Lee, J.Y. Free vibration analysis of functionally graded Bernoulli-Euler beams using an exact transfer matrix expression. *Int. J. Mech. Sci.* **2017**, *122*, 1–17. [[CrossRef](#)]
36. Lee, J.W.; Lee, J.Y. A transfer matrix method capable of determining the exact solutions of a twisted Bernoulli-Euler beam with multiple edge cracks. *Appl. Math. Model.* **2017**, *41*, 474–493. [[CrossRef](#)]

Disclaimer/Publisher's Note: The statements, opinions and data contained in all publications are solely those of the individual author(s) and contributor(s) and not of MDPI and/or the editor(s). MDPI and/or the editor(s) disclaim responsibility for any injury to people or property resulting from any ideas, methods, instructions or products referred to in the content.